

Study of Neutral Current Deep Inelastic ep Scattering at High x and Q^2

with the



Detector at HERA

ULRICH F. KATZ
UNIVERSITY OF BONN

ON BEHALF OF THE ZEUS COLLABORATION

CERN SEMINAR, 4 MARCH 1997

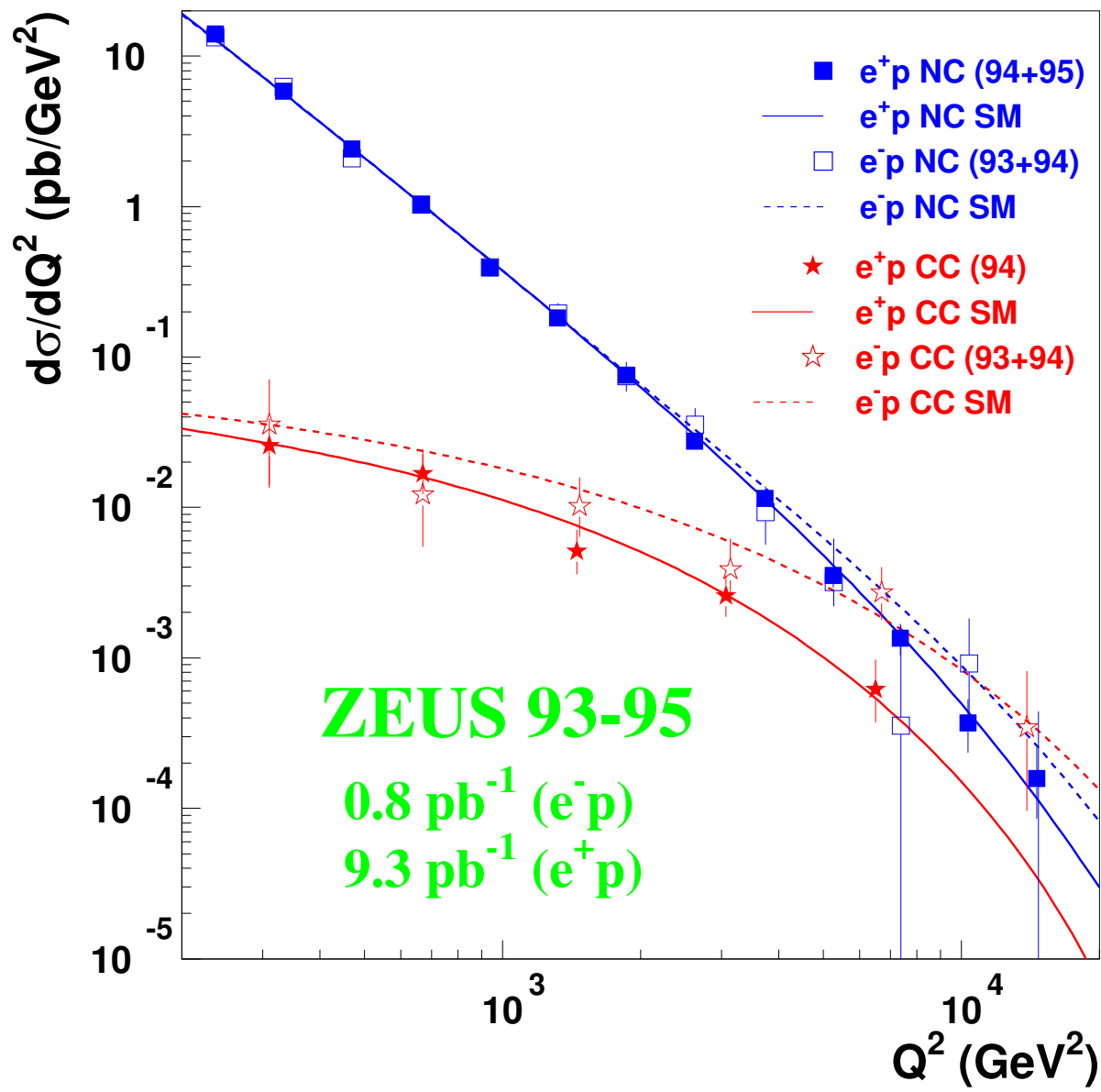
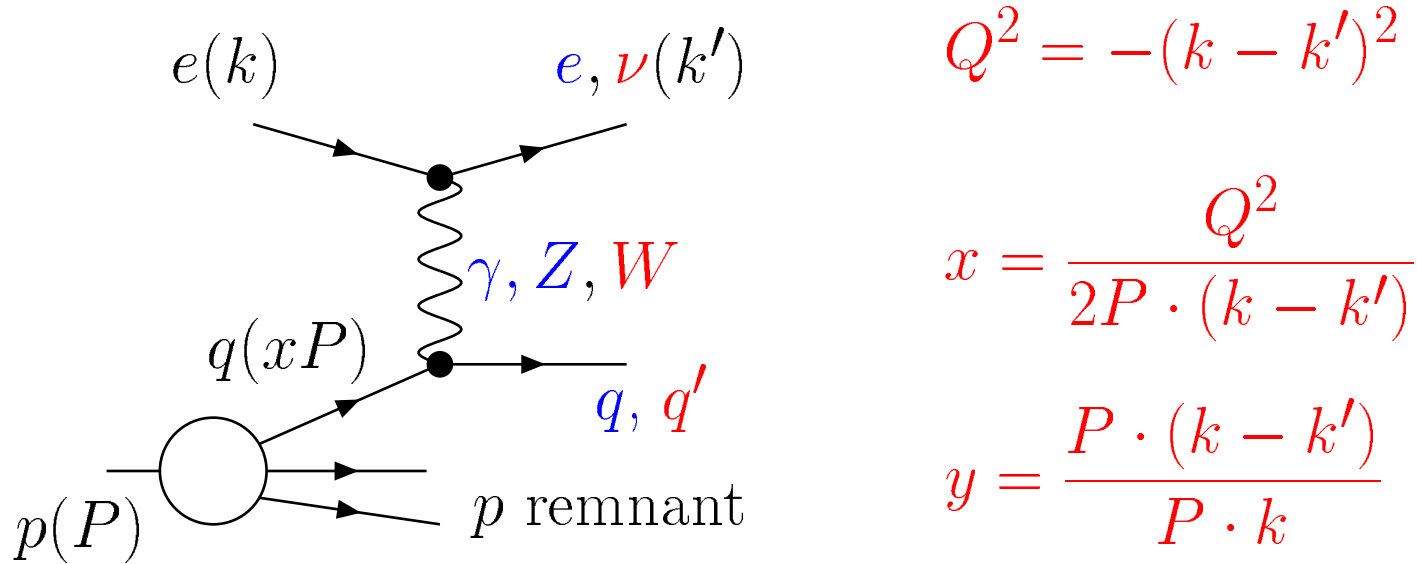
- Standard Model Deep Inelastic ep Scattering
- Neutral Current DIS Kinematics and Reconstruction
- Data Selection
- Final Data Sample
- Backgrounds
- Systematic Uncertainties from Theory and Experiment
- Significance Analysis
 - Search for an excess in the x spectrum
 - Search for an excess in the Q^2 spectrum
 - Likelihood of the (x, y) distribution
- Conclusions

ZEUS 1994–1996 integrated luminosity = 20.1 pb^{-1}

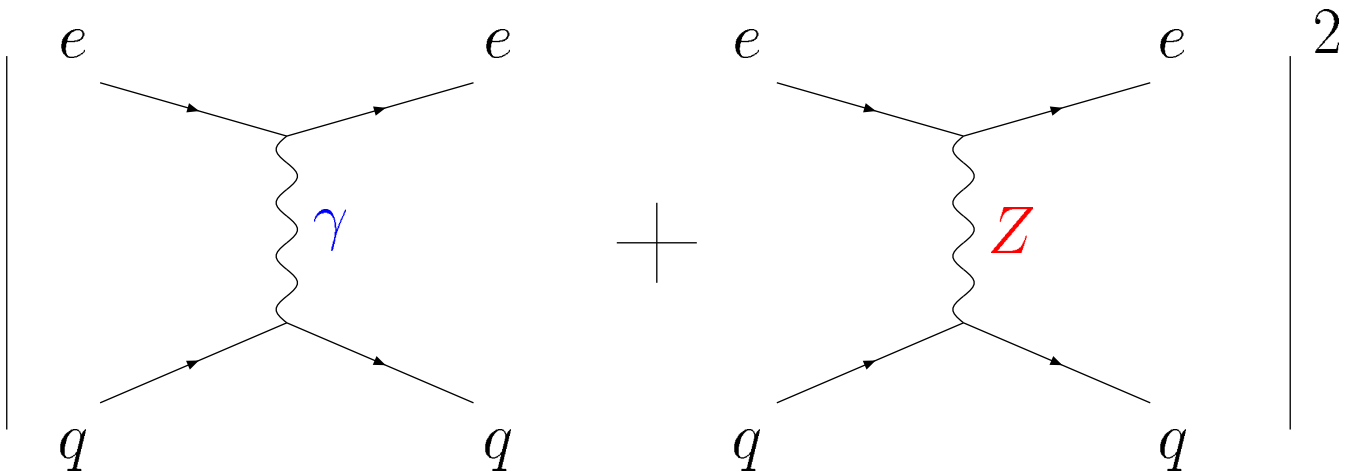
→ sensitive to $\sigma \sim 50 \text{ fb}$

$\sqrt{s} = 300 \text{ GeV}$, $x = 0.5 \rightarrow M = \sqrt{sx} = 212 \text{ GeV}$
 $Q^2 = 10000 \text{ GeV}^2 \rightarrow \text{spatial resolution} = 2 \cdot 10^{-16} \text{ cm}$

Deep Inelastic ep Scattering



Standard Model Reaction: t -channel γ or Z Exchange



$$\frac{d^2\sigma}{dx dQ^2} = \frac{2\pi\alpha^2}{x Q^4} \{ Y_+ \mathcal{F}_2(x, Q^2) - Y_- x \mathcal{F}_3(x, Q^2) \}$$

$$Y_{\pm} = 1 \pm (1 - y)^2$$

The structure functions \mathcal{F} are given by

$$\begin{pmatrix} \mathcal{F}_2(x, Q^2) \\ x \mathcal{F}_3(x, Q^2) \end{pmatrix} = x \sum_{q=\text{quarks}} \begin{pmatrix} C_2^q(Q^2) [q(x, Q^2) + \bar{q}(x, Q^2)] \\ C_3^q(Q^2) [q(x, Q^2) - \bar{q}(x, Q^2)] \end{pmatrix}$$

with coefficient functions

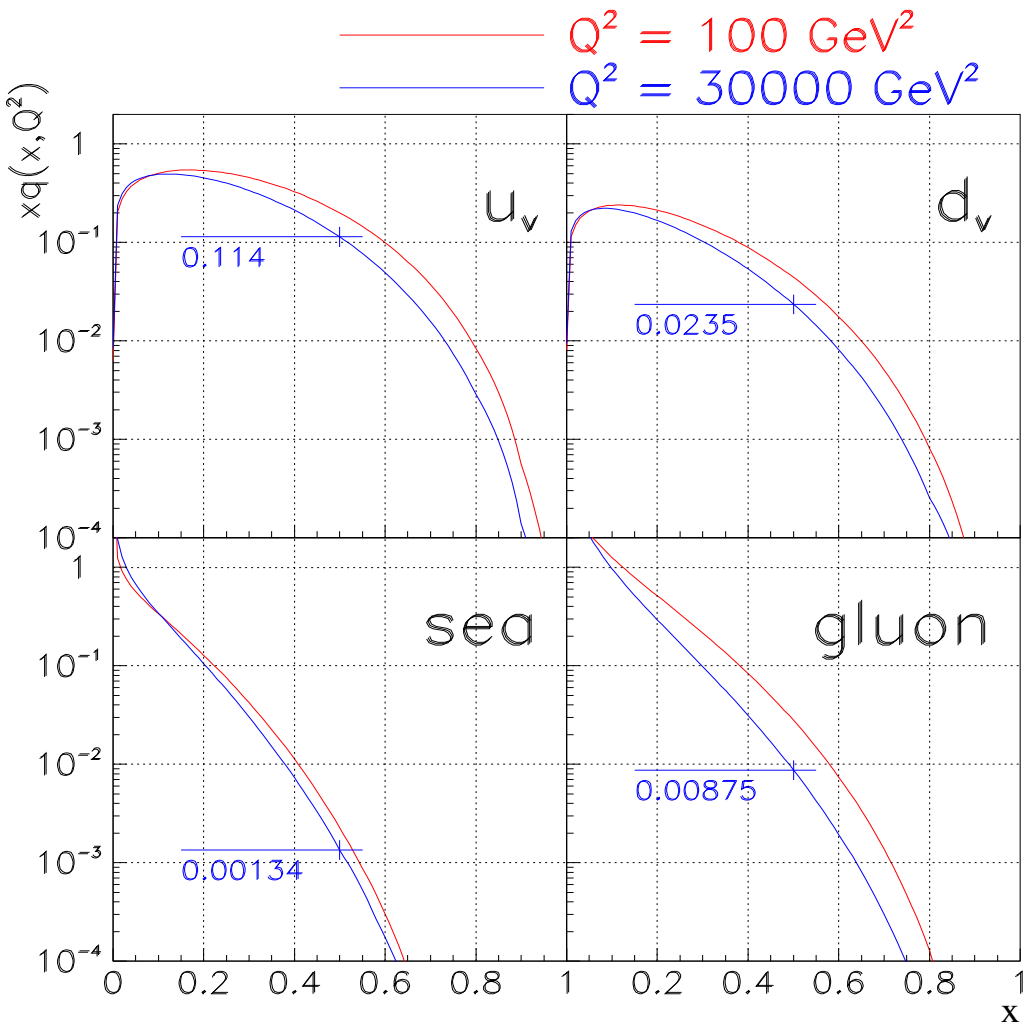
$$\begin{pmatrix} C_2^q(Q^2) \\ C_3^q(Q^2) \end{pmatrix} = \begin{pmatrix} e_q^2 & -2e_q v_q v_e \chi_Z + (v_q^2 + a_q^2)(v_e^2 + a_e^2) \chi_Z^2 \\ & -2e_q a_q a_e \chi_Z + (2v_q a_q)(2v_e a_e) \chi_Z^2 \end{pmatrix}$$

$$\chi_Z = \frac{1}{4 \sin^2 \theta_w \cos^2 \theta_w} \frac{Q^2}{Q^2 + M_Z^2}$$

Experimental Input to Cross Section Prediction

The NC DIS cross section depends on:

- well measured Electroweak parameters α , θ_w , M_Z
→ uncertainties at the 0.25 % level.
- the quark structure in the proton, $q(x, Q^2)$, $\bar{q}(x, Q^2)$.

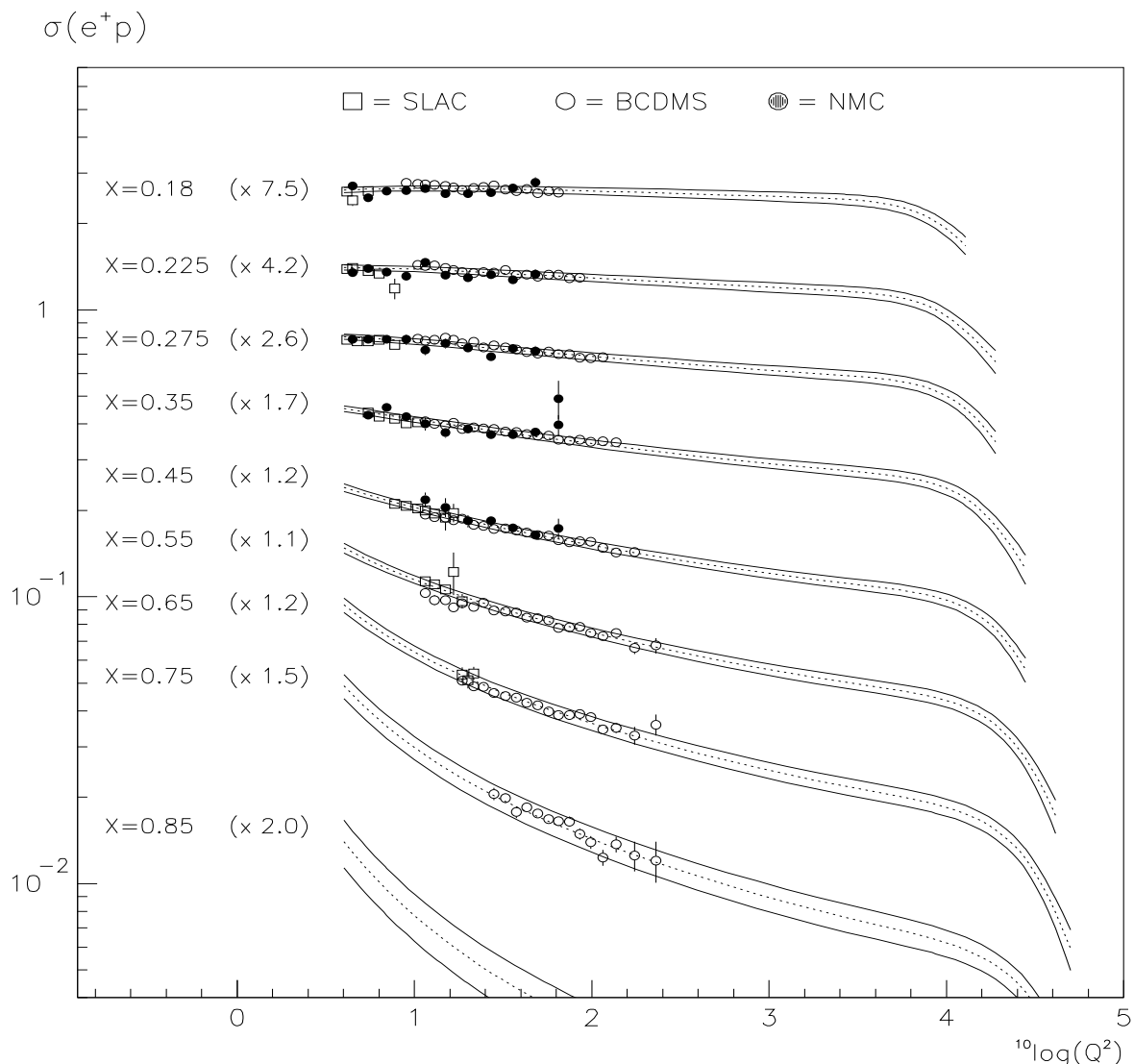


At high x , Q^2 :

- Quark densities are determined from a NLO DGLAP evolution of parton densities at higher x and lower Q^2 .
- The u quark dominates the cross section since $q \gg \bar{q}$ and $u > d$ and $|e_u| = 2|e_d|$.

ZEUS DGLAP Fit to SLAC, BCDMS, and NMC Data

$$\sigma(e^+ p) \equiv \frac{xQ^4}{2\pi\alpha^2 Y_+} \frac{d^2\sigma_{NC}^{e^+ p}}{dx dQ^2} = F_2 - \frac{y^2}{Y_+} F_L - \frac{Y_-}{Y_+} x F_3$$

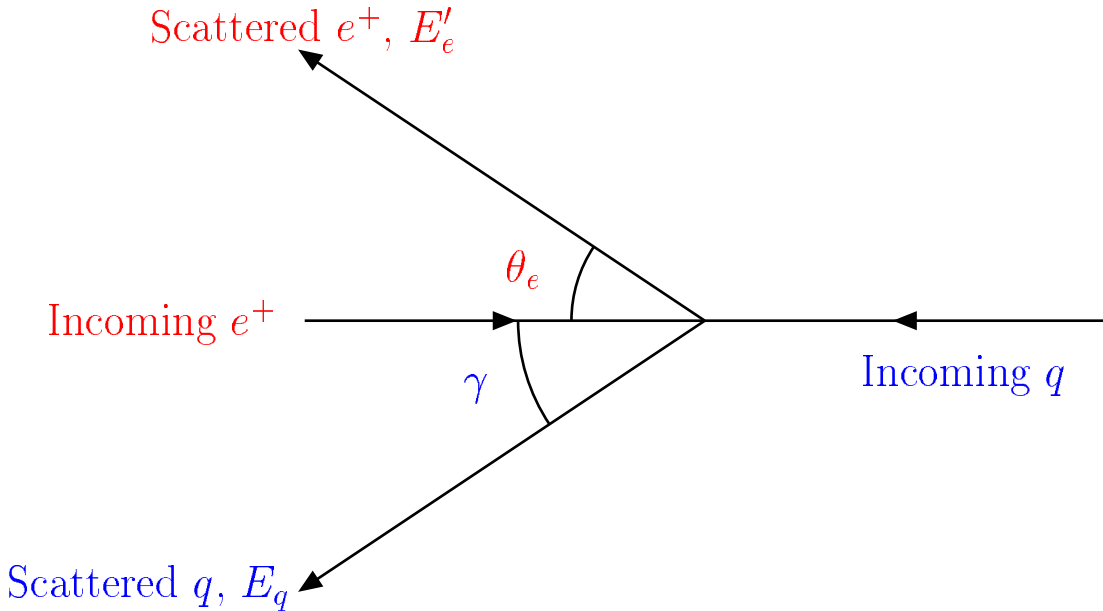


Error Bands include:

- SLAC, BCDMS, NMC statistical and systematic errors
- the effect of varying α_s between 0.112 and 0.122

NC DIS cross section predictions at high x , Q^2
accurate to $\approx 6.5\%$

Kinematic Reconstruction



ZEUS uses the **Double Angle Method** :

$$x_{\text{DA}} = \frac{E_e}{E_p} \frac{\sin \gamma}{(1 - \cos \gamma)} \frac{\sin \theta}{(1 - \cos \theta)}$$

$$y_{\text{DA}} = \frac{\sin \theta_e (1 - \cos \gamma)}{\sin \gamma + \sin \theta_e - \sin(\gamma + \theta_e)}$$

$$Q_{\text{DA}}^2 = s x_{\text{DA}} y_{\text{DA}}$$

insensitive to
energy scale

The **Electron Method** is used as a cross-check:

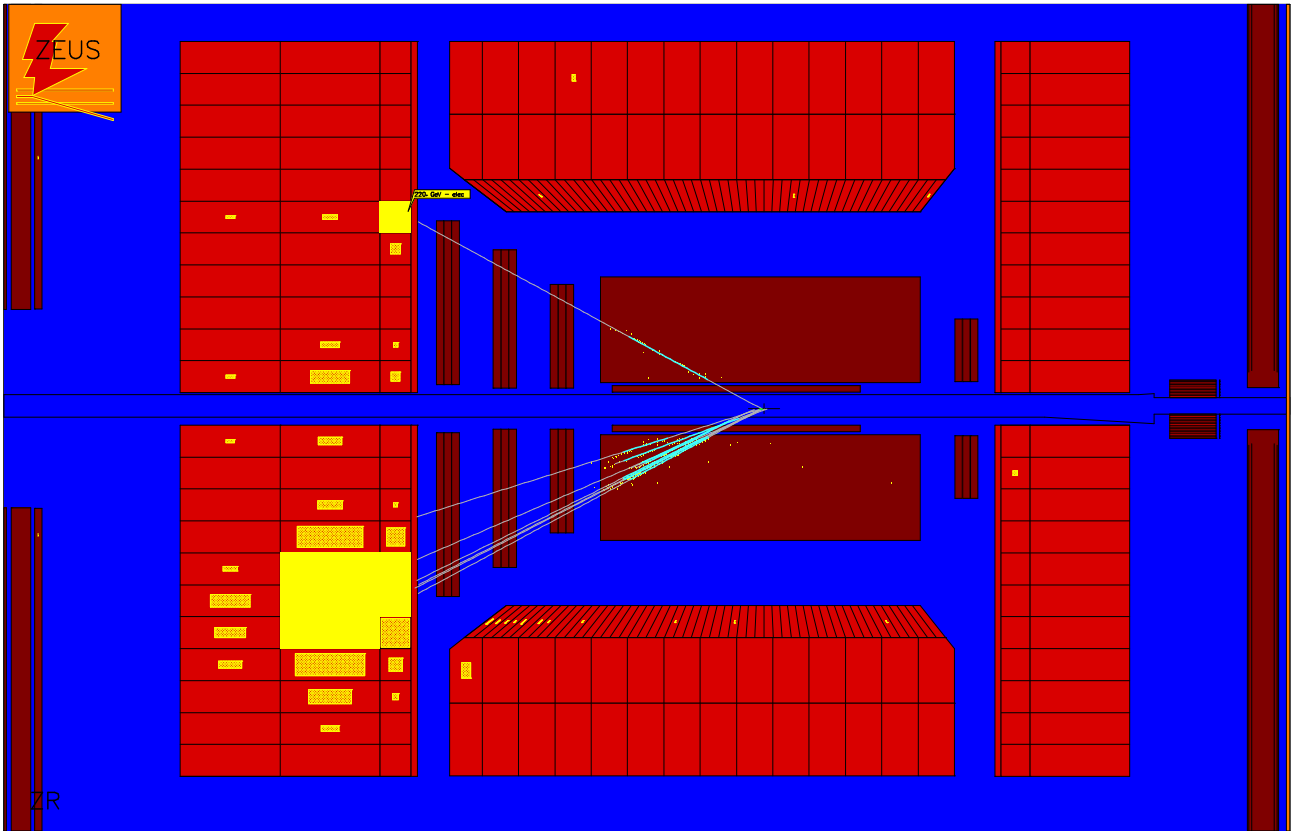
$$x_e = \frac{E_e}{E_p} \frac{E'_e (1 + \cos \theta_e)}{2E_e - E'_e (1 - \cos \theta_e)}$$

$$y_e = 1 - \frac{E'_e}{2E_e} (1 - \cos \theta_e)$$

$$Q_e^2 = s x_e y_e$$

does not use
hadronic final
state

The ZEUS Detector



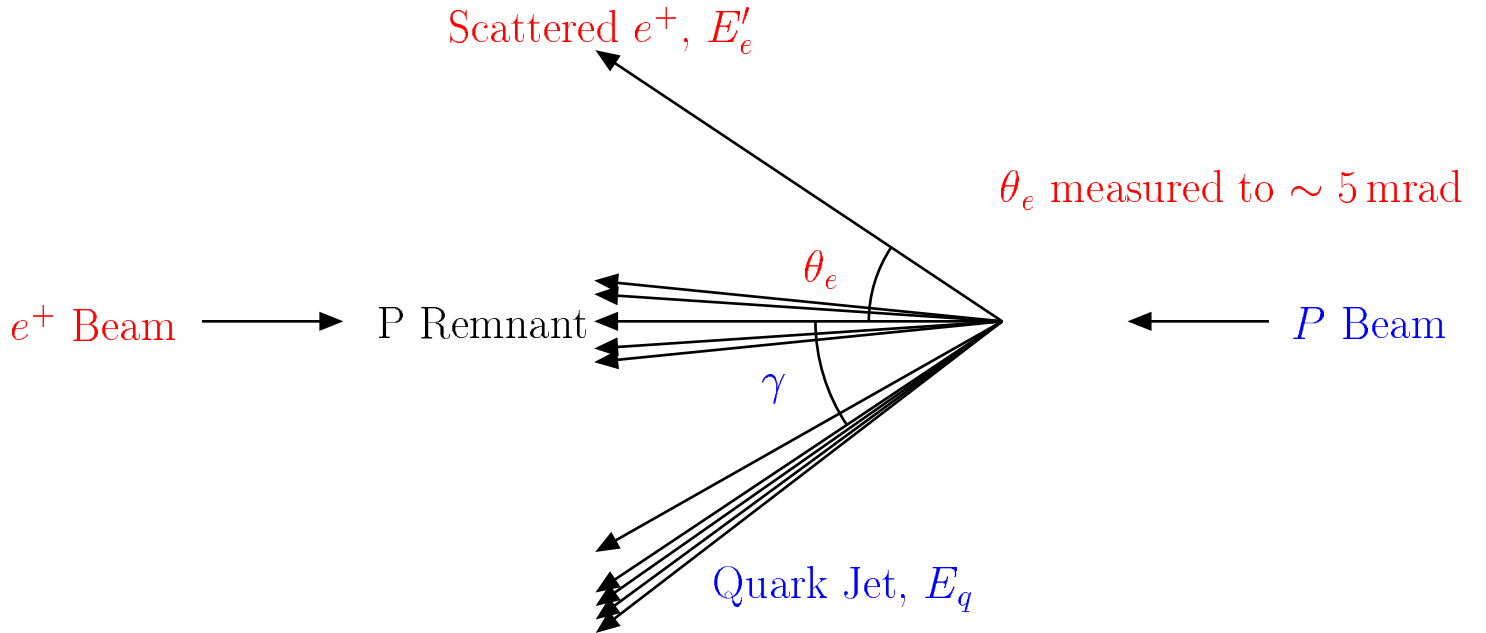
- Calorimeter (CAL):

- Energy resolution: $\frac{\sigma(E)}{E} = \begin{cases} 18\%/\sqrt{E} & \text{em.} \\ 35\%/\sqrt{E} & \text{hadronic} \end{cases}$
- Energy scale uncertainty: $\pm 3\%$

- Central tracking detector (CTD):

- Angular acceptance: $15^\circ < \theta < 164^\circ$
- Resolution: $\frac{\sigma(p_t^{\text{track}})}{p_t^{\text{track}}} = [0.005 p_t^{\text{track}} (\text{GeV})] \oplus 0.016$
(for full length tracks)

Reconstruction of Event Variables



$(E^i, p_X^i, p_Y^i, p_Z^i)$ = measured 4-momentum in calorimeter cell i .

$$p_t = \sqrt{\left(\sum_i p_X^i\right)^2 + \left(\sum_i p_Y^i\right)^2}$$

$$E - p_Z = \sum_i (E^i - p_Z^i)$$

$$E_t = \sum_i \sqrt{(p_X^i)^2 + (p_Y^i)^2}$$

\sum_i =
sum over all cells

$$(p_t)_{\text{had}} = \sqrt{\left(\sum_i' p_X^i\right)^2 + \left(\sum_i' p_Y^i\right)^2}$$

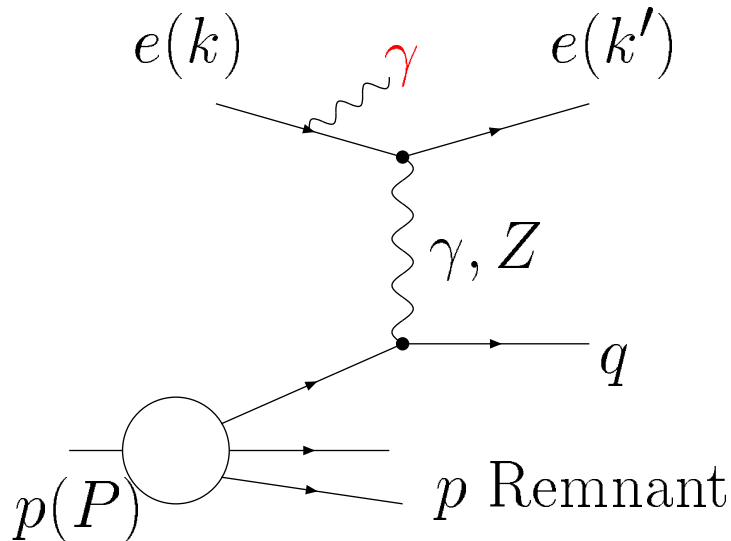
$$(E - p_Z)_{\text{had}} = \sum_i' (E^i - p_Z^i)$$

$$\cos \gamma_{\text{raw}} = \frac{(p_t)_{\text{had}}^2 - (E - p_Z)_{\text{had}}^2}{(p_t)_{\text{had}}^2 + (E - p_Z)_{\text{had}}^2}$$

$$E_q = \frac{(p_t)_{\text{had}}}{\sin \gamma}$$

\sum_i' =
sum over all cells
excluding e^+

Initial State Radiation and Kinematic Reconstruction



Initial State Radiation (ISR):

- mostly collinear with e beam
- can escape detection
- effectively reduces E_e
- events with ISR photons with $E_\gamma \gtrsim 7.5 \text{ GeV}$ rejected by cuts

$$f_\gamma = \frac{E_\gamma}{E_e} = \text{fractional energy carried by } \gamma$$

$$\begin{aligned} x_{\text{DA}} &= x \frac{1}{1 - f_\gamma} \\ Q_{\text{DA}}^2 &= Q^2 \frac{1}{(1 - f_\gamma)^2} \end{aligned}$$

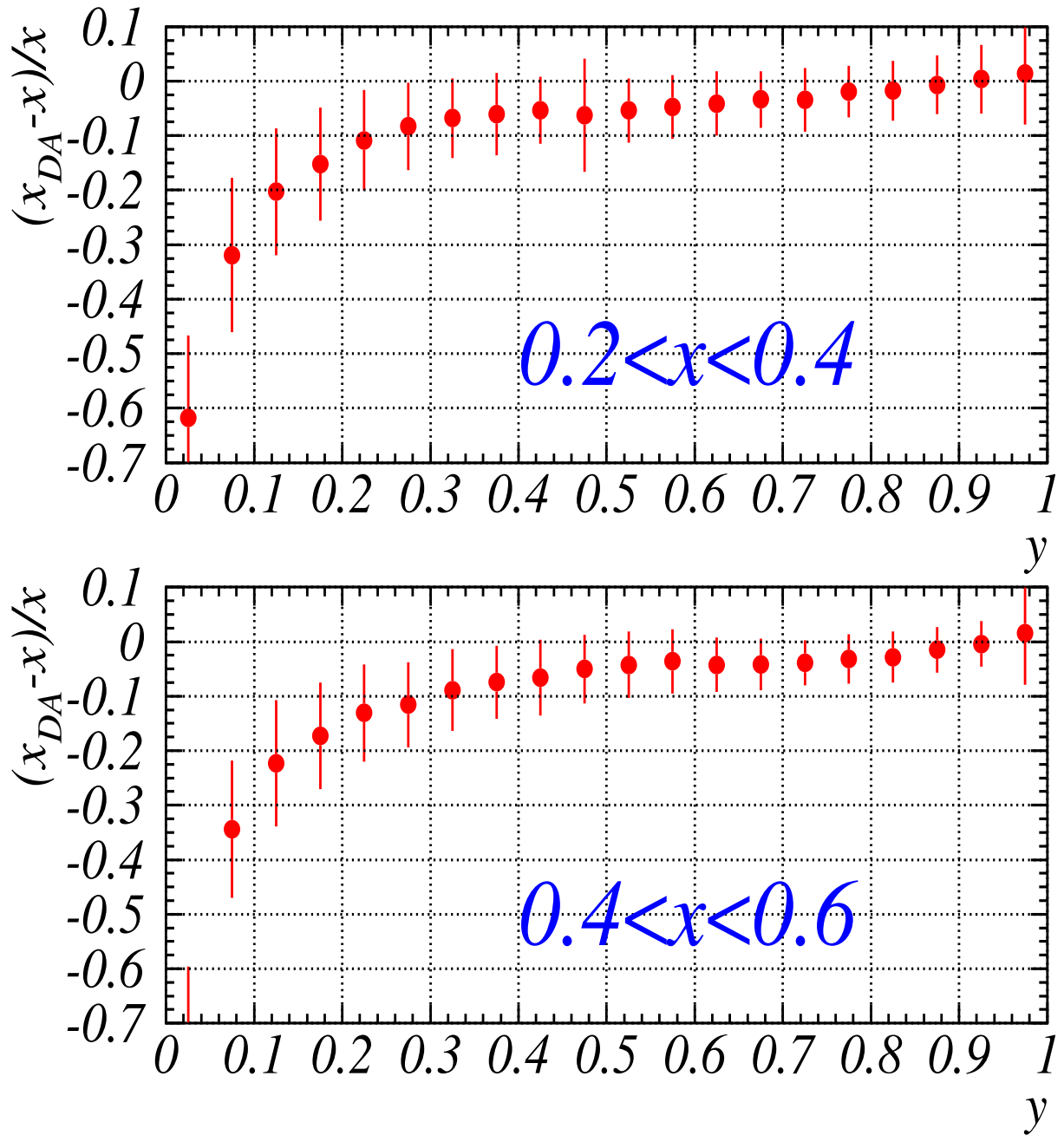
$$\begin{aligned} x_e &= x \frac{(1 - f_\gamma/y_e)}{(1 - f_\gamma)} \\ Q_e^2 &= Q^2 \frac{1}{(1 - f_\gamma)} \end{aligned}$$

Average shifts of true kinematic variables due to ISR
for events passing all cuts and having $0.4 < x < 0.6$, $y > 0.25$

$$\langle \delta x_{\text{DA}} \rangle = \left\langle \frac{x_{\text{DA}} - x}{x} \right\rangle = +1.7\% \quad \langle \delta Q_{\text{DA}}^2 \rangle = \left\langle \frac{Q_{\text{DA}}^2 - Q^2}{Q^2} \right\rangle = +2.5\%$$

$$\langle \delta x_e \rangle = \left\langle \frac{x_e - x}{x} \right\rangle = -2.5\% \quad \langle \delta Q_e^2 \rangle = \left\langle \frac{Q_e^2 - Q^2}{Q^2} \right\rangle = +1.8\%$$

Shifts and Resolution of Uncorrected x_{DA}

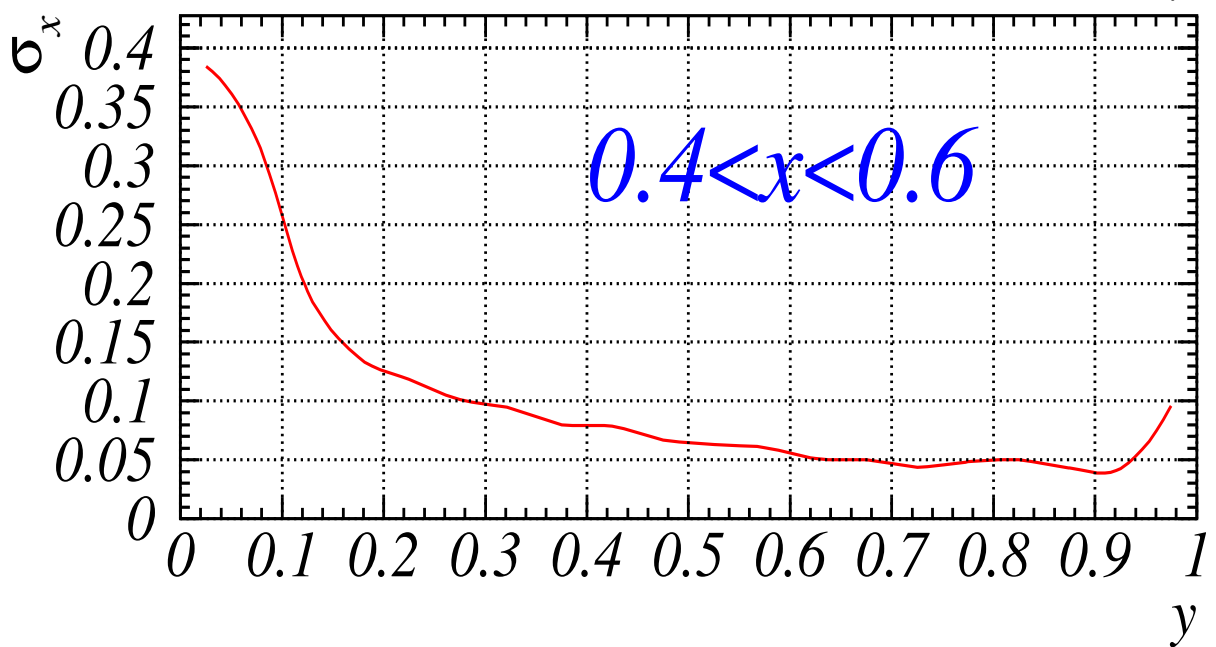
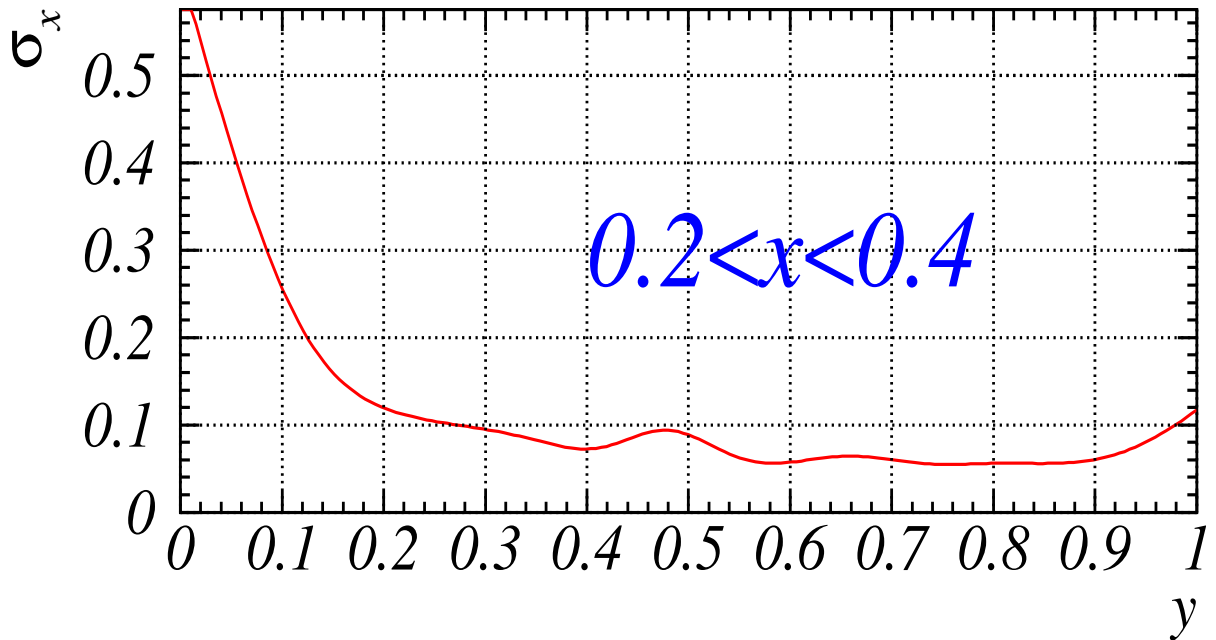


Problem at low $y \leftrightarrow$ small γ :

- At small γ , $\gamma_{\text{raw}} > \gamma_{\text{true}}$ on average.
- the uncorrected x_{DA} yields a biased x measurement.

We correct γ event by event.

Resolution of the Corrected x_{DA}



$$\sigma_x = \text{RMS of } \frac{x_{\text{DA}} - x}{x}$$

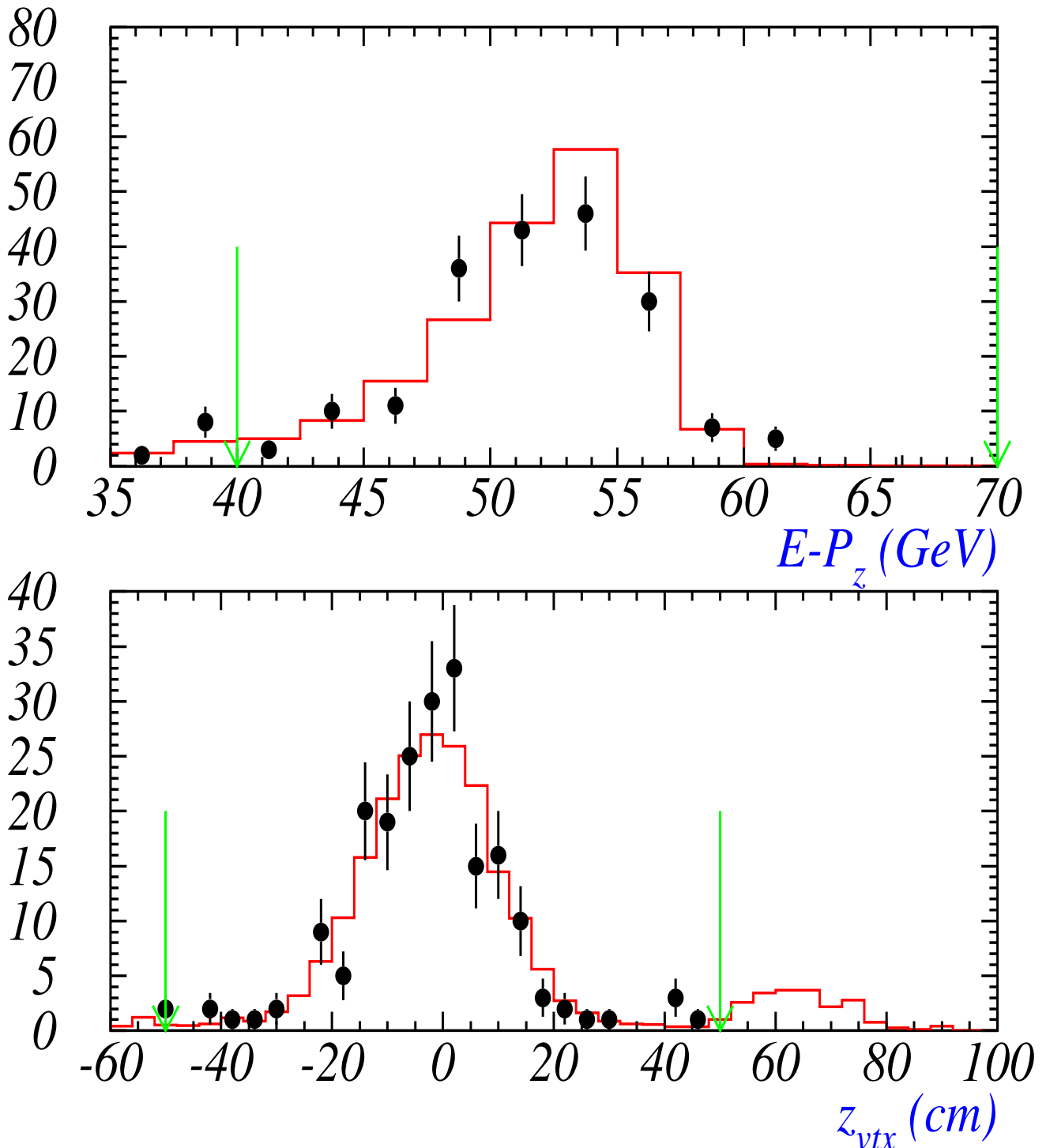
Effects of **ISR** are included.

Data Selection

Efficiencies are evaluated using NC MC events
with $Q_{\text{true}}^2 > 5000 \text{ GeV}^2$

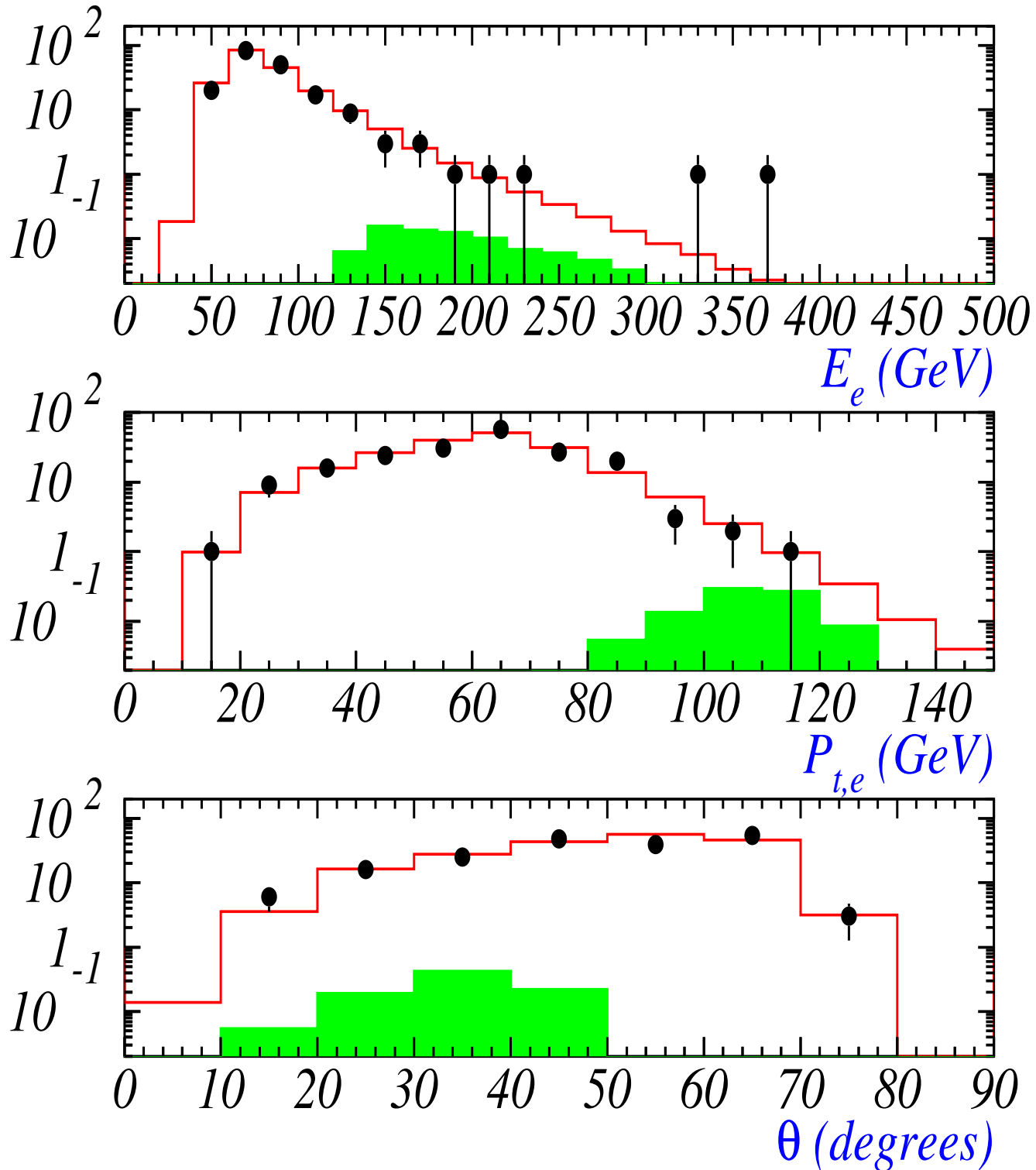
Selection	Efficiency
Vertex found	100.0 %
$ Z_{\text{vtx}} < 50 \text{ cm}$	94.9 %
$40 \text{ GeV} < E - p_Z < 70 \text{ GeV}$ (lower cut rejects photoproduction or hard ISR)	92.0 %
Positron with $E'_e > 20 \text{ GeV}$ identified in CAL	89.4 %
Positron isolation $E_{\text{cone}}^{R=0.8} < 5 \text{ GeV}$	87.2 %
If $\theta_e > 17.2^\circ$:	
track–cluster match (DCA < 10 cm)	85.7 %
If $\theta_e < 17.2^\circ$:	
$p_{t,e} > 30 \text{ GeV}$	83.9 %
$E - p_Z > 44 \text{ GeV}$ (tighter Photoproduction rejection)	83.8 %
Reject events with 2 isolated e.m. clusters (Compton rejection)	83.4 %
$Q_{\text{DA}}^2 > 5000 \text{ GeV}^2$	81.5 %

Data/MC Comparison for $E - P_z$ and Vertex Z-Position.



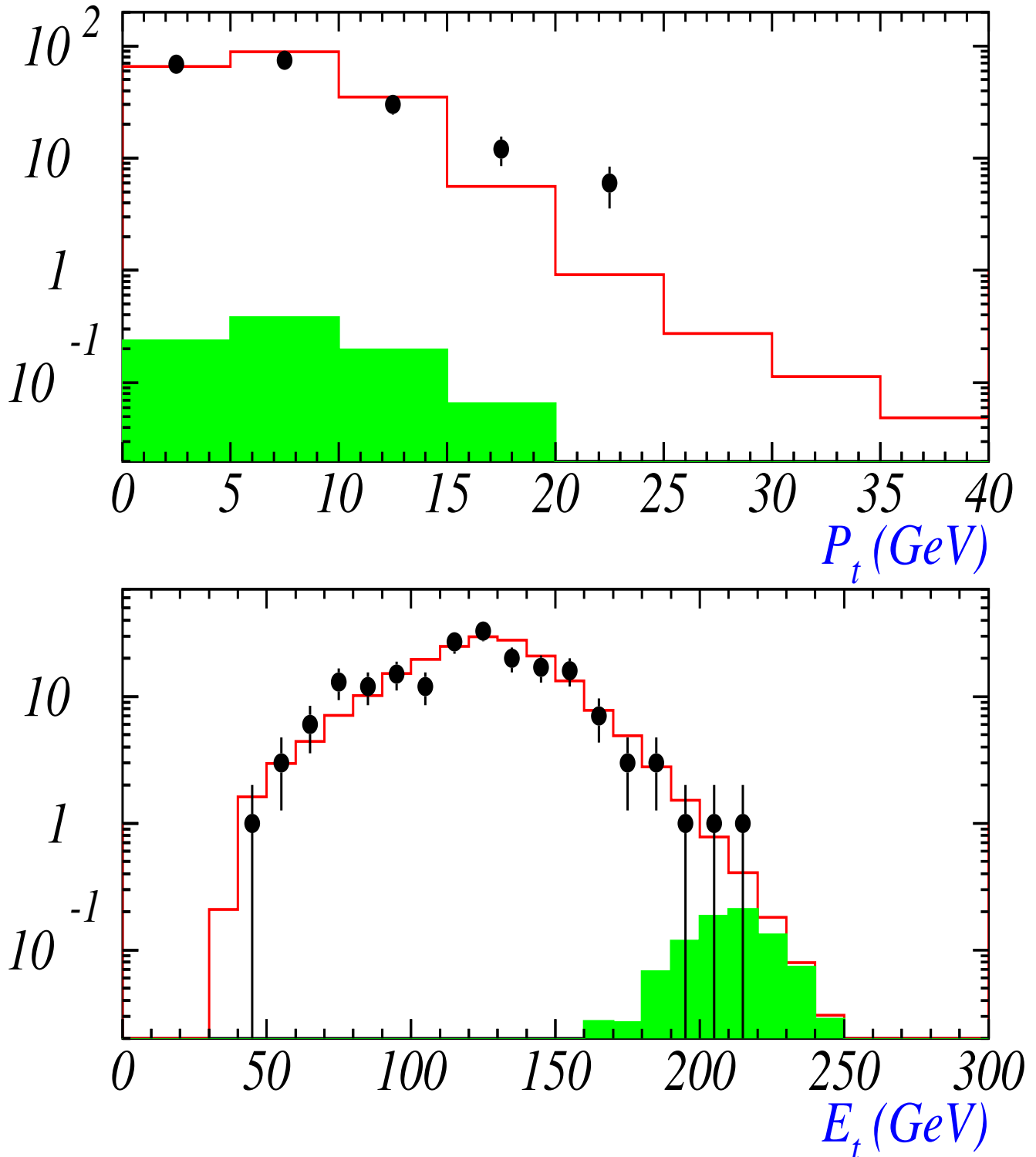
Data is plotted only for $|z_{vtx}| < 50$ cm .

Data/MC Comparison for Final-State Positron



Green indicates MC distributions
for $x_{\text{DA}} > 0.55$ and $y_{\text{DA}} > 0.25$.

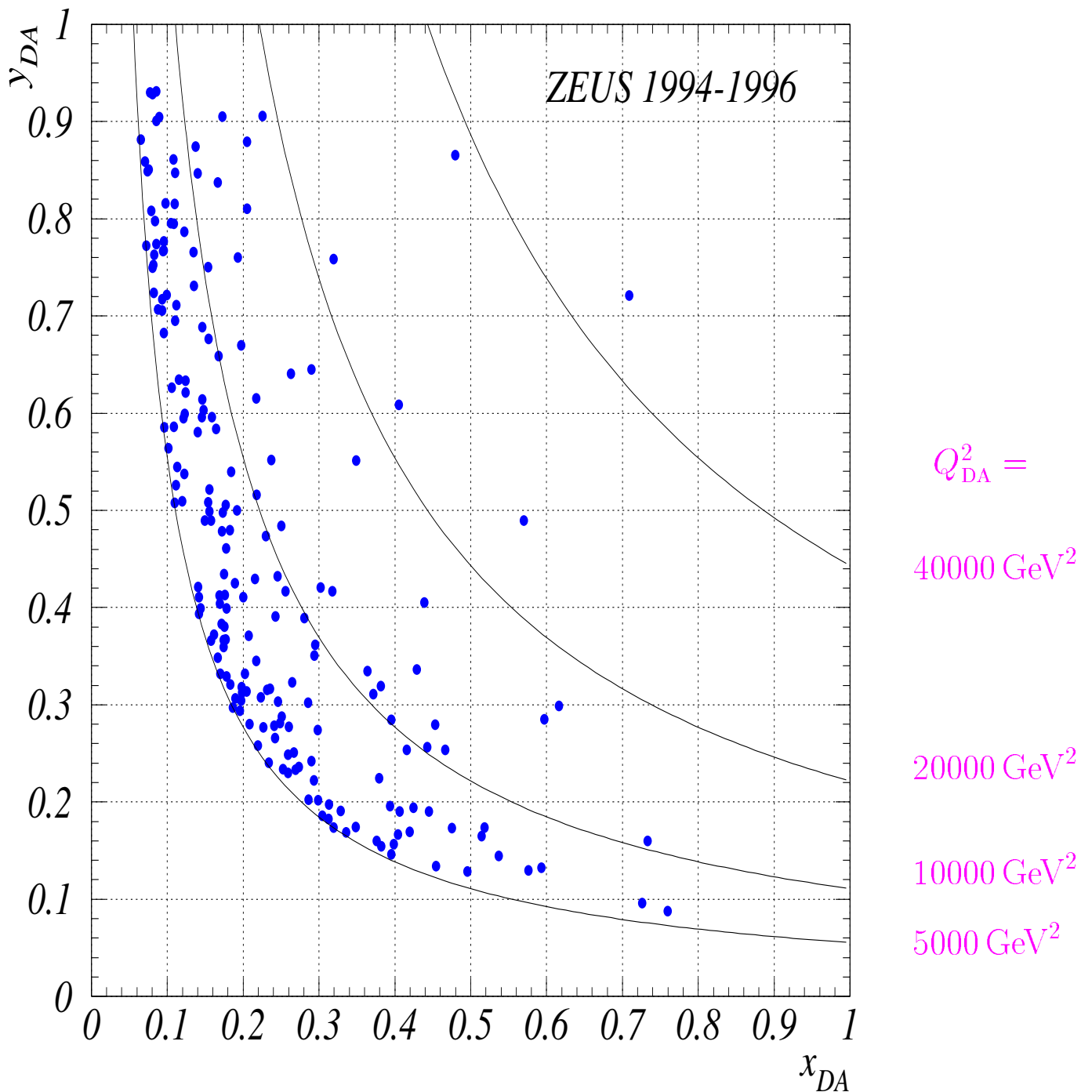
Data/MC Comparison for p_t and Energy



Green indicates MC distributions
for $x_{\text{DA}} > 0.55$ and $y_{\text{DA}} > 0.25$.

Final Data Sample

The final sample consists of 191 events



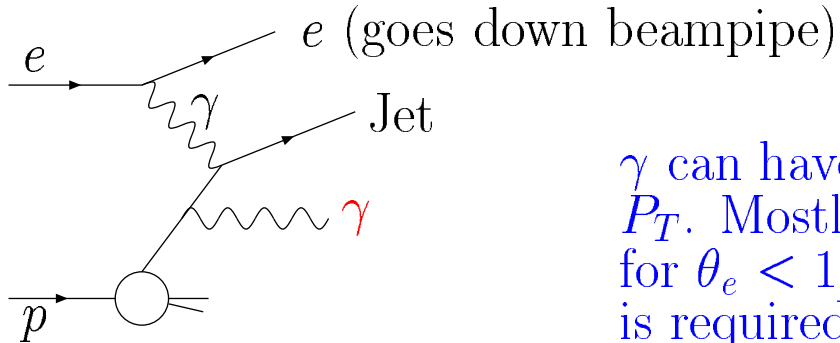
	x_{DA} range									
y_{DA} range	0.05 — 0.15	0.15 — 0.25	0.25 — 0.35	0.35 — 0.45	0.45 — 0.55	0.55 — 0.65	0.65 — 0.75	0.75 — 0.85	0.85 — 0.95	0.95 — 1.00
0.95 – 1.00	0.15	0.015	0.033	0.013	0.0055	0.0015	0.0012			
0.85 – 0.95	8.8 9	1.2 3	0.32	0.10	0.028 1	0.01	0.0034			
0.75 – 0.85	12 16	2.5 4	0.50 1	0.15	0.050	0.011	0.0039			
0.65 – 0.75	13 10	3.7 3	0.86	0.26	0.082	0.022	0.0054 1	0.0020		
0.55 – 0.65	15 12	6.1 3	1.65 3	0.46 1	0.15	0.046	0.0090	0.0024		
0.45 – 0.55	12 6	11 13	2.5 1	0.85	0.28	0.084 1	0.0208	0.0032		
0.35 – 0.45	4.6 3	18 17	5.5 6	1.75	0.52	0.16	0.0403	0.0093		
0.25 – 0.35		18 23	11 6	3.74 7	1.19 1	0.34 2	0.1104	0.0175	0.0066	
0.15 – 0.25		2.2 1	14 15	9.6 10	3.32 3	1.2	0.2784 1	0.0717	0.0077	
0.05 – 0.15				1.3 1	2.14 3	1.6 2	0.9052 1	0.3022 1	0.1216	

ZEUS 1994–1996 Selected Events

Event Date	11-Oct-94	03-Nov-95	12-Sep-96	12-Oct-96	21-Nov-96
E_t [GeV]	123.	217.	193.	204.	187.
p_t [GeV]	8.9	8.2	2.9	2.2	10.2
$E - p_Z$ [GeV]	47.8	53.2	49.7	50.2	49.1
E_q [GeV]	67.4	235.	270.	151.	276.
γ_{raw} [degrees]	69.0	28.1	19.9	40.7	19.7
E'_e [GeV]	324.	220.	149.	366.	134.
θ_e [degrees]	11.9	27.8	39.3	15.4	41.1
$[x_{\text{DA}}]_{\text{raw}}$	0.468	0.541	0.535	0.668	0.515
$[y_{\text{DA}}]_{\text{raw}}$	0.868	0.503	0.330	0.733	0.316
$(Q_{\text{DA}}^2)_{\text{raw}}$ [10^4 GeV^2]	3.67	2.45	1.59	4.42	1.47
γ [degrees]	67.6	26.7	17.3	38.6	17.0
x_{DA}	0.480	0.570	0.617	0.709	0.597
δx_{DA}	0.035	0.029	0.054	0.034	0.053
y_{DA}	0.865	0.490	0.299	0.721	0.285
δy_{DA}	0.008	0.010	0.017	0.008	0.017
Q_{DA}^2 [10^4 GeV^2]	3.75	2.52	1.66	4.61	1.54
$\delta[Q_{\text{DA}}^2]$ [10^4 GeV^2]	0.26	0.07	0.05	0.16	0.04
x_e	0.525	0.536	0.562	0.605	0.443
δx_e	0.048	0.048	0.102	0.060	0.063
y_e	0.854	0.505	0.319	0.752	0.350
δy_e	0.018	0.024	0.039	0.021	0.032
Q_e^2 [10^4 GeV^2]	4.05	2.44	1.62	4.10	1.40
$\delta[Q_e^2]$ [10^4 GeV^2]	0.31	0.11	0.09	0.30	0.07

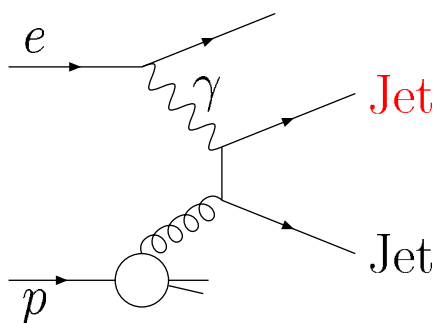
Backgrounds

Prompt Photon Production:

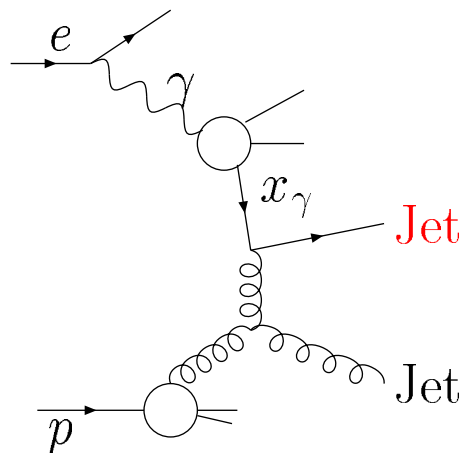


γ can have large energy, and P_T . Mostly a background for $\theta_e < 17.2^\circ$ where no track is required.

Photoproduction of Dijets:



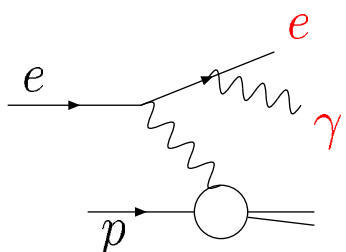
Direct Photoproduction



Resolved Photoproduction

Background when jet satisfies
electron requirements

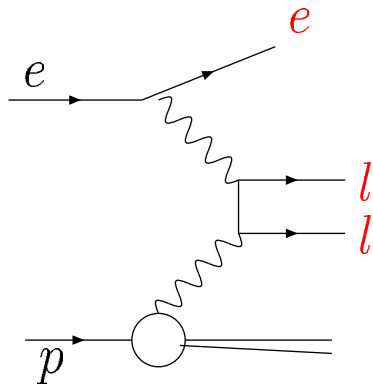
QED Compton:



e , γ can be produced with large transverse momentum

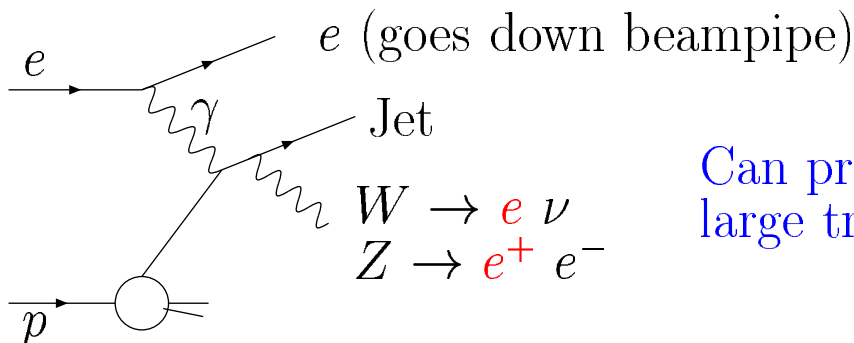
Backgrounds — continued

Dilepton Photoproduction:



l can have large P_T .
Background if e or l misidentified

Weak Boson Production:



Can produce e with
large transverse momentum

Expected cross sections for backgrounds
($<$ indicates 90% confidence level upper limit)

Background Process	Cross-section [fb]	Cross-section [fb]
$\gamma p \rightarrow \gamma X$	0.28	0.28
$\gamma p \rightarrow \text{dijets}$	< 1.8	< 1.8
$ep \rightarrow e\gamma X$	< 0.2	< 0.2
$\gamma\gamma \rightarrow ll$	< 0.1	< 0.1
$W \rightarrow e\nu$	< 0.5	< 0.5
Accepted NC DIS	165	46

Systematic errors in SM predictions

Luminosity uncertainty	2.3%
Electroweak parameters	0.25%
Radiative corrections	2%
Evaluated with HERACLES and HECTOR	
ISR E_γ spectrum in LUMI monitor agrees well with MC.	
Detector simulation	4.4%
$\sim 2\%$ for $y_{\text{DA}} > 0.2$	
4 – 7% for $y_{\text{DA}} > 0.5$	

Effects included:

- variation of $\pm 3\%$ in the FCAL, BCAL energy scales
- smearing of the electron scattering angle (5 mrad)
- variation in the electron finding efficiency
 - variation of HAC fraction of electron candidate
 - variation of lateral energy profiles of the electron
 - variation of non-electron energy in the cone
 - variation of track-cluster matching angles
 - variation of track momentum resolution

Systematic errors in SM predictions — continued

Structure Functions 6.5%

Uncertainties from structure function fit:

Fixed-target experimental uncertainties	$\pm 6.2\%$
$0.112 < \alpha_s < 0.122$	$\pm 1.9\%$

Cross checks on SF uncertainties include:

$10\% <$ strange fraction $< 30\%$	small
Uncertainties in charm evolution	$< 0.5\%$
GRV94, MRSA, CTEQ3 comparison	$\pm 2.0\%$
GRV94 NLO versus LO	$+1.0\%$
High- x gluon (CDF inspired, CTEQ4 HJ)	$+1.9\%$

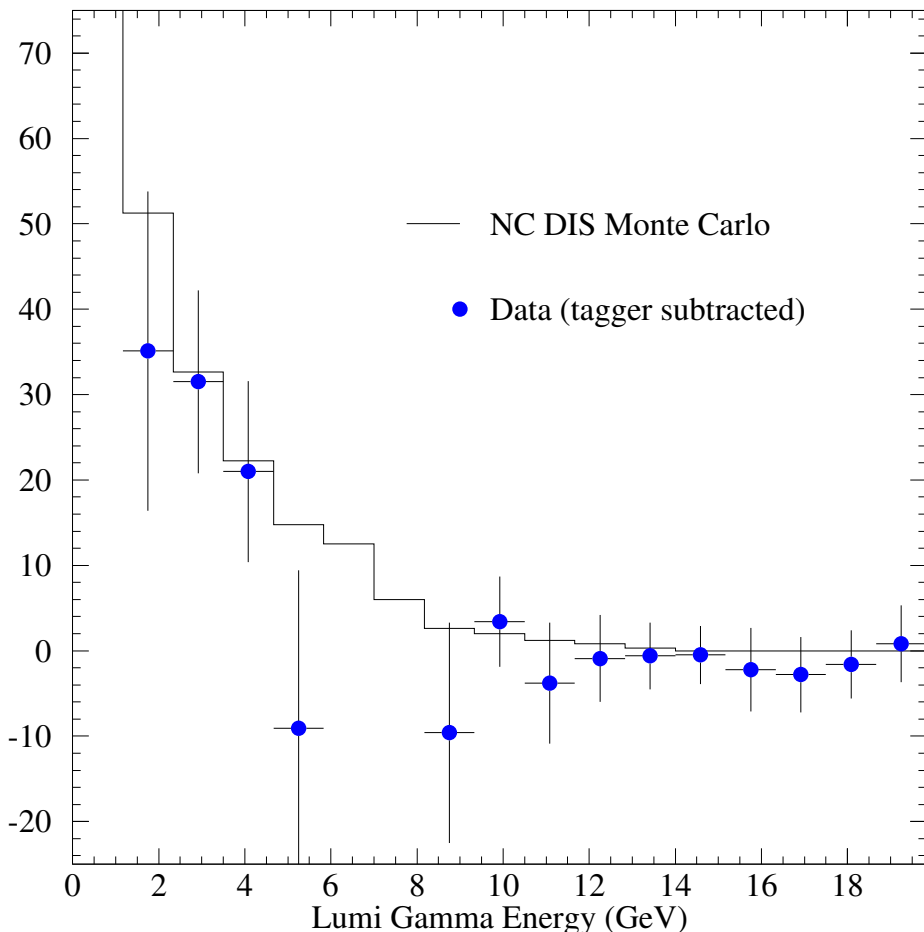
Summary of systematic errors in SM predictions

for $x > 0.55$ and $y > 0.25$

Luminosity measurement	2.3%
Electroweak parameters	0.25%
Radiative corrections	2%
Detector simulation	4.4%
Structure Functions	6.5%
Total	8.4%

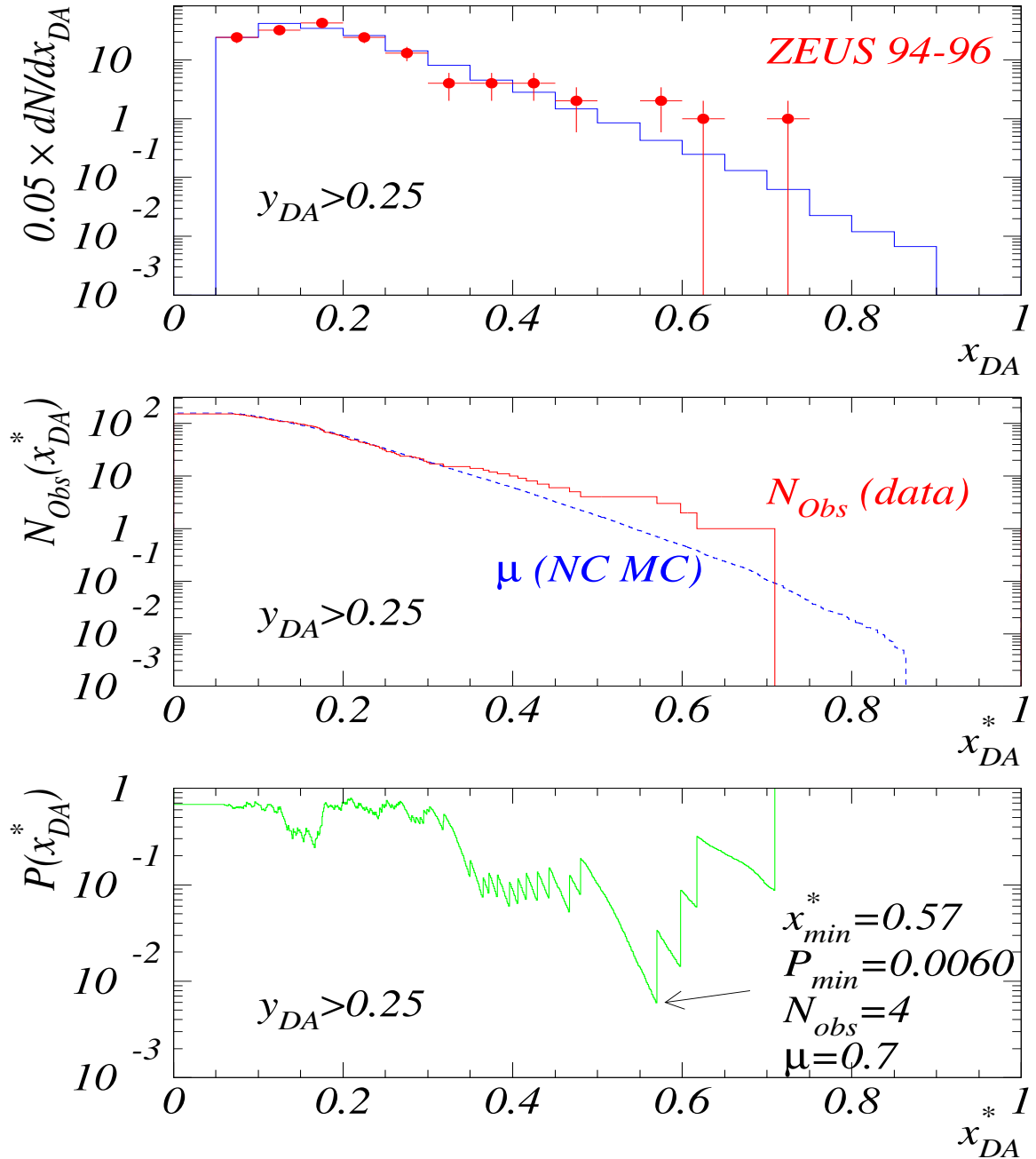
Comparison between data and MC of the ISR photon energy spectrum

- Data/MC comparison of E_γ spectrum in the luminosity monitor photon calorimeter (LUMI- γ).
- Select NC events with $Q_{\text{DA}}^2 > 400 \text{ GeV}^2$ and $E_{\text{LUMI}-\gamma} > 1.2 \text{ GeV}$ (460 events out of 5630).
- Subtract rate of random bremsstrahlung coincidences using events in which the positron is tagged in the 44 m ($E_\gamma < 6 \text{ GeV}$) or 35 m ($E_\gamma \approx 7 - 25 \text{ GeV}$) calorimeters.
- The resulting E_γ spectrum agrees well with the MC prediction, with 88 ± 24 events measured and 105 expected in the range $1.2 \text{ GeV} < E_{\text{LUMI}-\gamma} < 4.8 \text{ GeV}$.



Significance Analysis

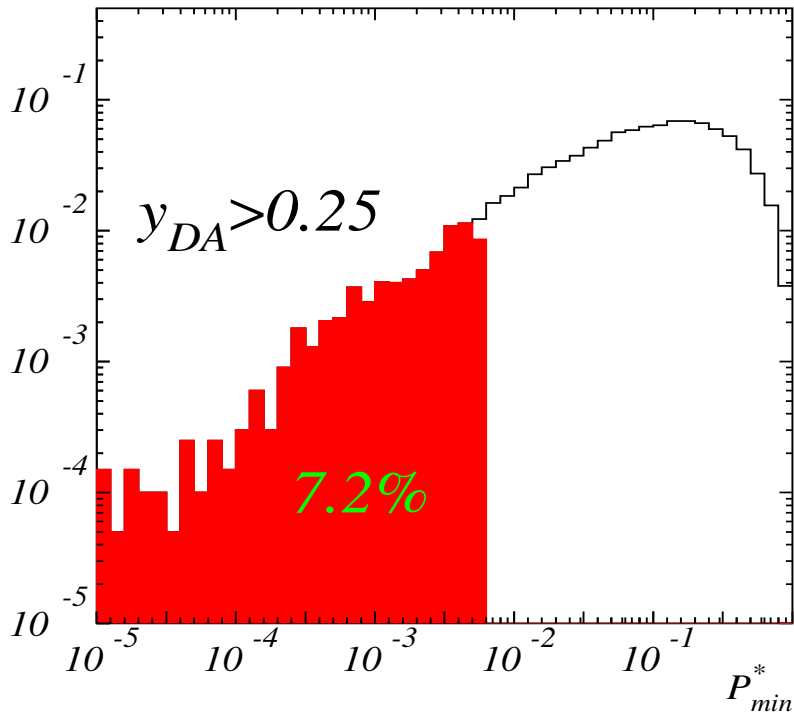
Excess in x



$$N_{obs}(x_{DA}^*) = \int_{x_{DA}^*} dx_{DA} dN/dx_{DA}$$

$$\mathcal{P}(x_{DA}^*) = \sum_{n=N_{obs}}^{\infty} e^{-\mu} \frac{\mu^n}{n!}$$

Excess in x — continued



Minimal Poisson probabilities of the x_{DA} distributions for different y_{DA} cuts

y_{DA} range	$\mathcal{P}_{\min}(x_{\text{DA}}^*) [\%]$	x_{DA}^*	N_{obs}	μ	$P_{\text{SM}} [\%]$
$y_{\text{DA}} > 0.05$	1.61	0.708	4	0.95	16.0
$y_{\text{DA}} > 0.15$	2.57	0.708	2	0.25	23.0
$y_{\text{DA}} > 0.25$	0.60	0.569	4	0.71	7.2
$y_{\text{DA}} > 0.35$	3.38	0.708	1	0.034	26.6
$y_{\text{DA}} > 0.45$	1.32	0.569	2	0.17	12.7
$y_{\text{DA}} > 0.55$	0.96	0.708	1	0.010	9.5
$y_{\text{DA}} > 0.65$	0.50	0.708	1	0.005	5.0

$\mathcal{P}_{\min}(x_{\text{DA}}^*)$ = the minimal probability

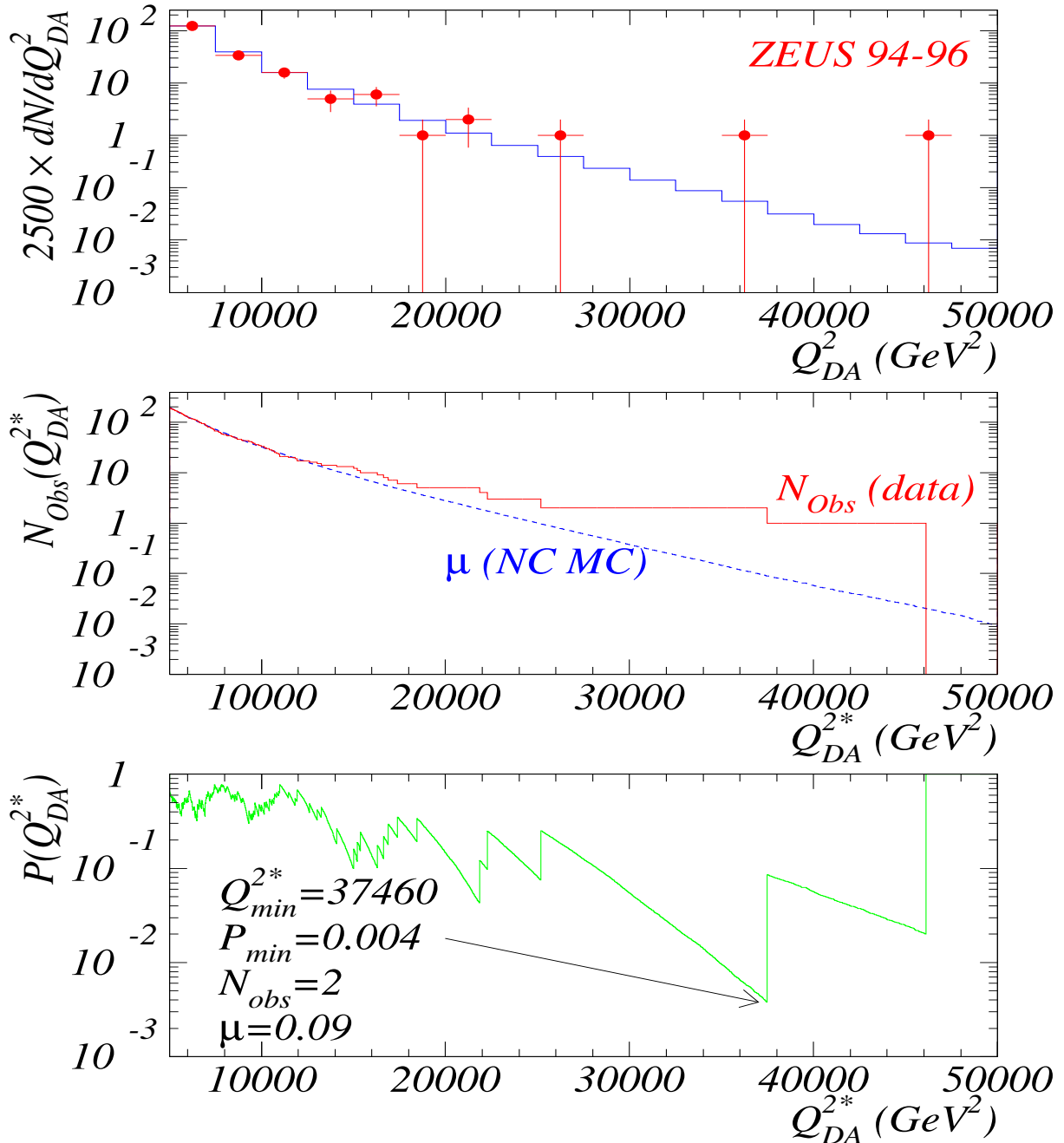
x_{DA}^* = the value of x_{DA} where it occurs

N_{obs} = number of events observed with $x_{\text{DA}} > x_{\text{DA}}^*$

μ = expected number of events with $x_{\text{DA}} > x_{\text{DA}}^*$

P_{SM} = prob. that a simulated experiment yields a lower $\mathcal{P}_{\min}(x_{\text{DA}}^*)$ than observed

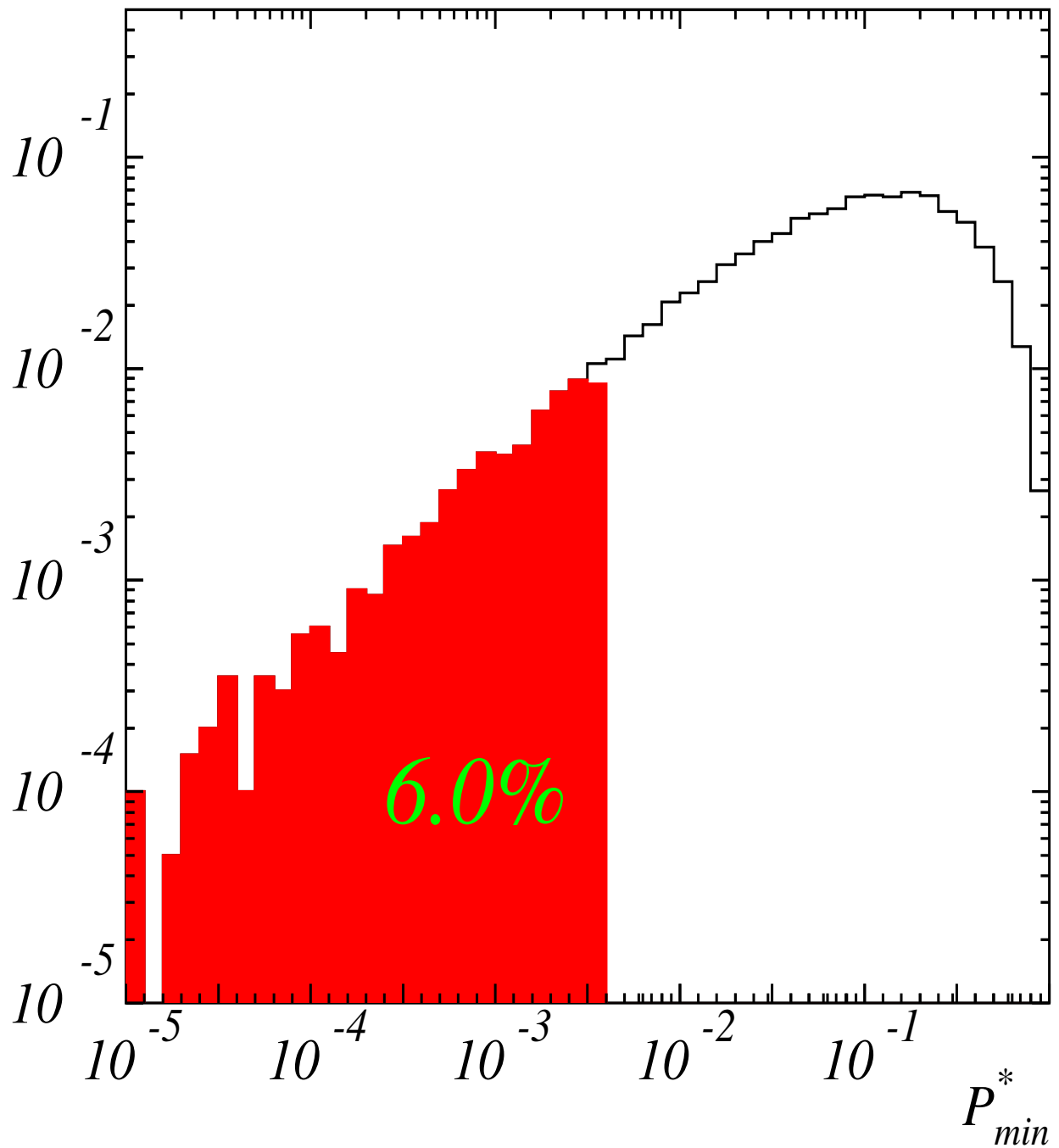
Excess in Q^2



$$N_{\text{obs}}((Q_{\text{DA}}^2)^*) = \int_{(Q_{\text{DA}}^2)^*} dx_{\text{DA}} dN/dx_{\text{DA}}$$

$$\mathcal{P}((Q_{\text{DA}}^2)^*) = \sum_{n=N_{\text{obs}}}^{\infty} e^{-\mu} \frac{\mu^n}{n!}$$

Excess in Q^2 – continued



The probability for a simulated experiment to obtain $\mathcal{P}_{min}((Q_{\text{DA}}^2)^*) < 0.004$ is 6.0%.

2–Dimensional Likelihood Test

- Divide x - y plane into 10×10 grid
- Assign Poisson probability to i^{th} bin

$$\mathcal{P}_i = e^{-\mu_i} \frac{\mu_i^{N_i}}{N_i!} \quad \begin{aligned} N_i &= \text{Number observed} \\ \mu_i &= \text{Number expected} \end{aligned}$$

- Form likelihood over a subset of bins \mathcal{R}

$$\mathcal{L}_{\mathcal{R}} = \prod_{i \in \mathcal{R}} \mathcal{P}_i$$

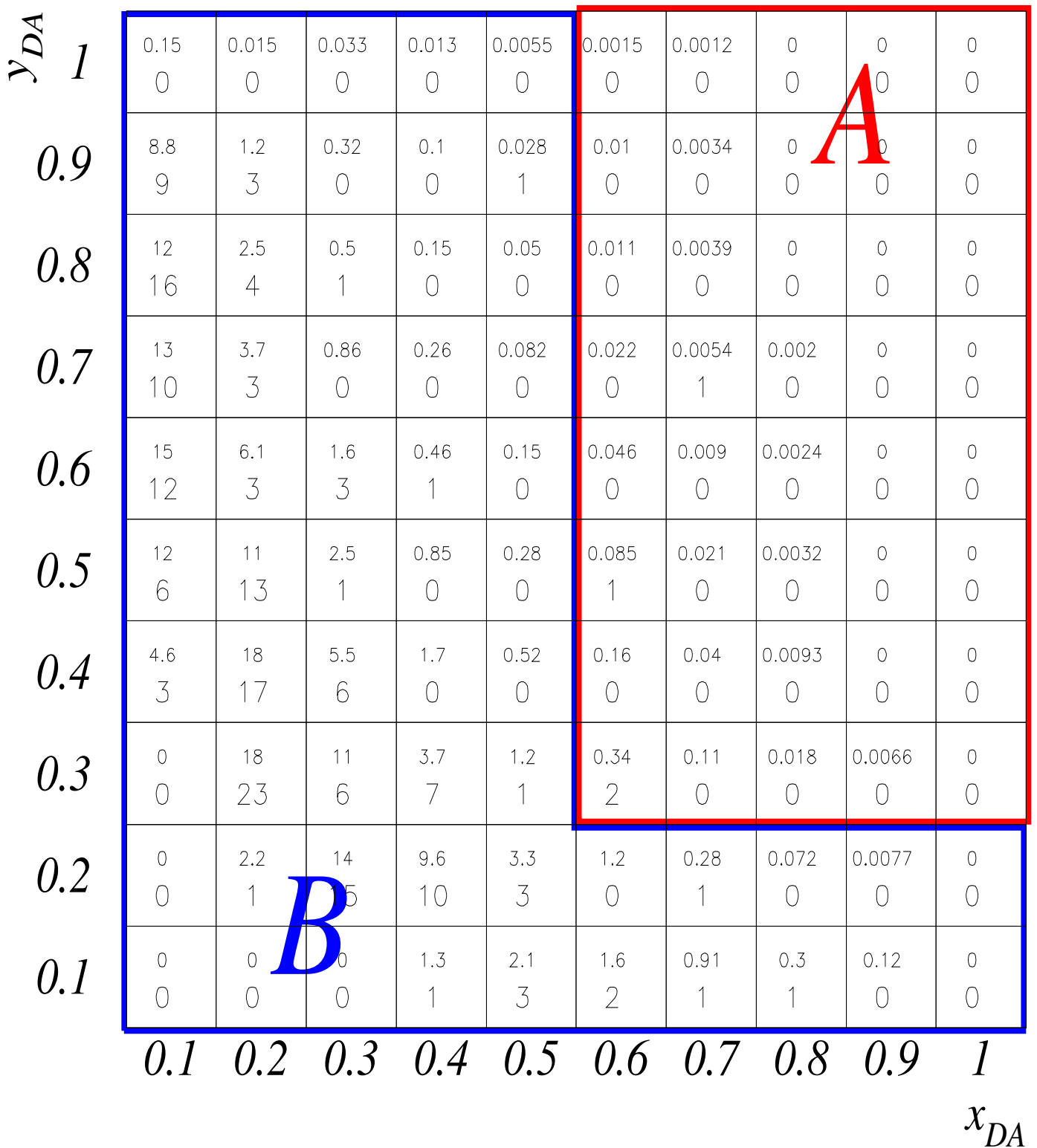
- Evaluate the significance by performing many Monte Carlo experiments

$$\mathcal{L}_{\mathcal{R}} = \prod_{i \in \mathcal{R}} \mathcal{P}_i^{(m)} \quad \text{for } m^{\text{th}} \text{ experiment}$$

- Significance \equiv Probability ($\mathcal{L}_{\mathcal{R}} \leq \mathcal{L}_{\mathcal{R}}^{\text{obs}}$)

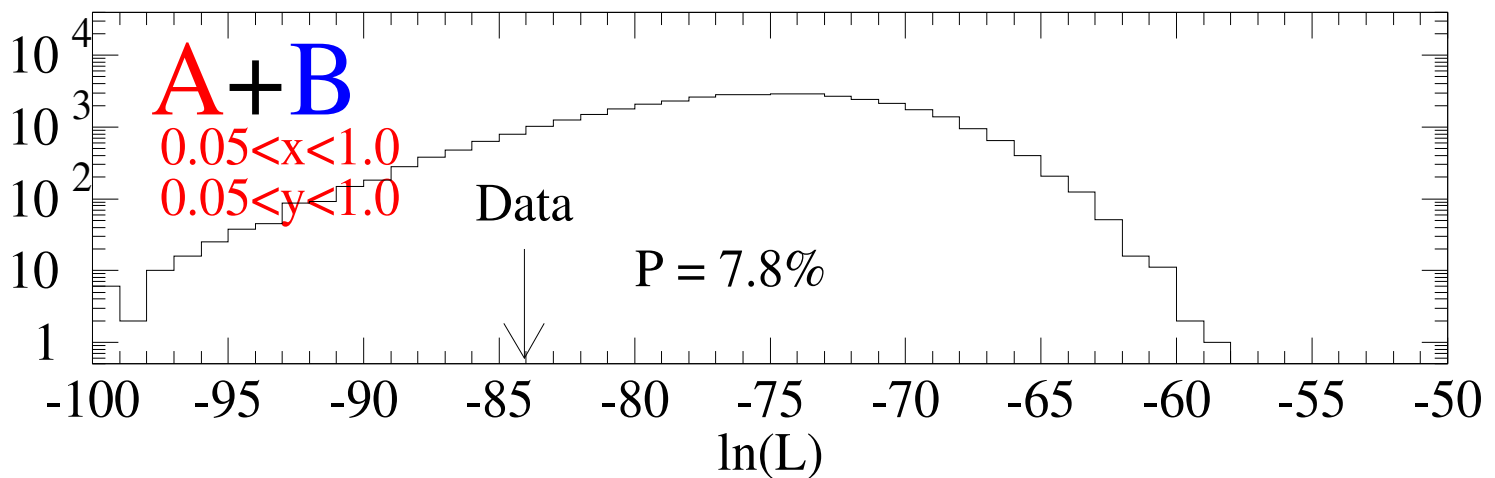
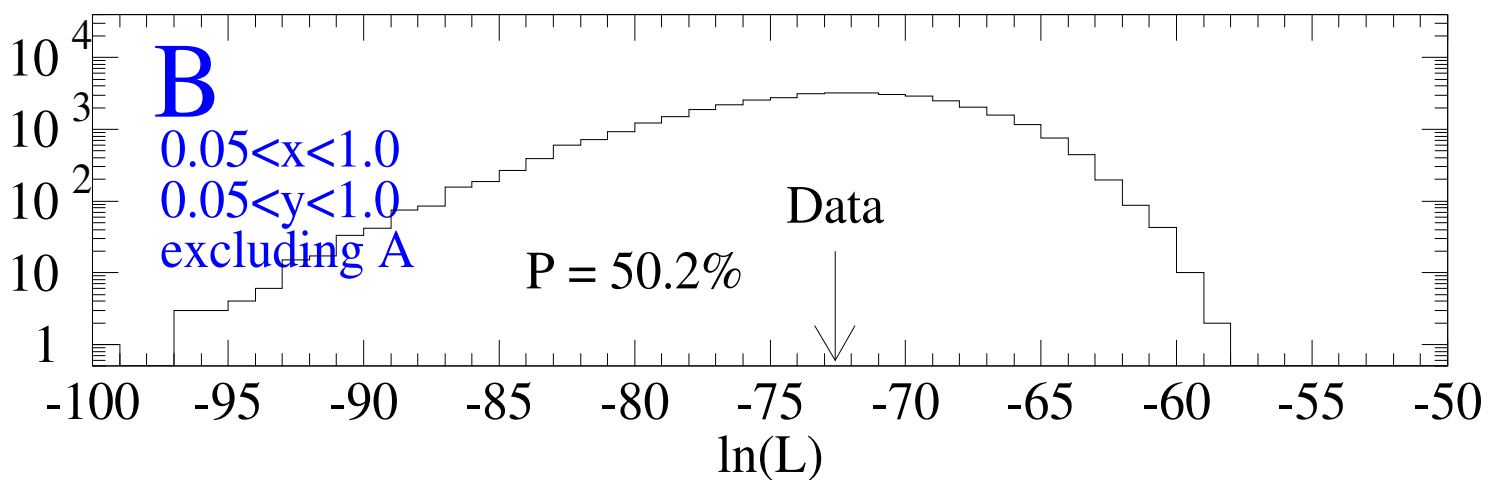
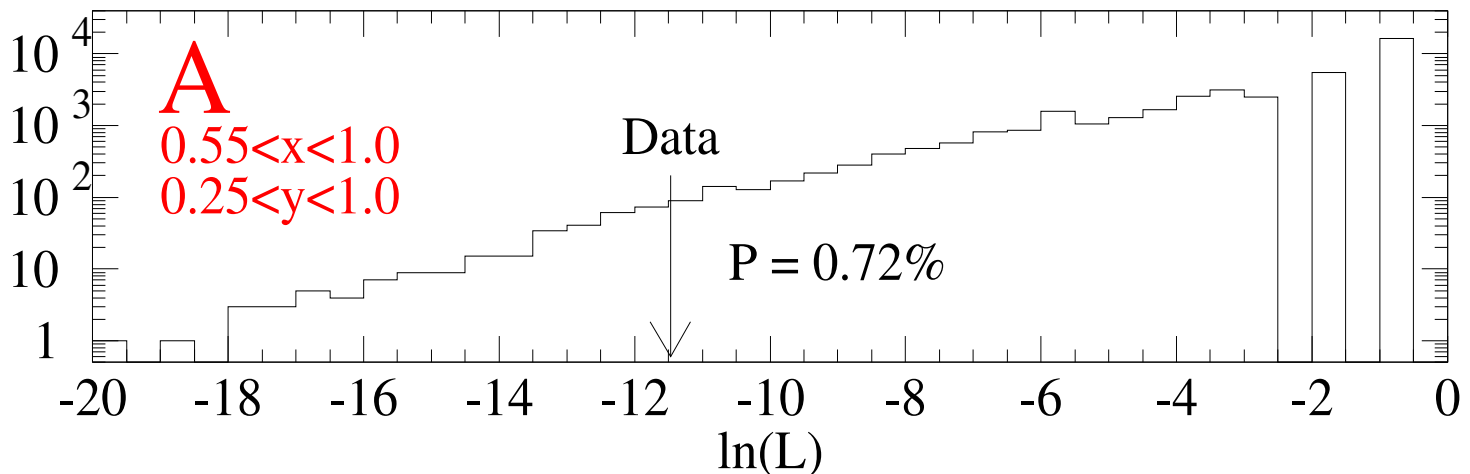
2-Dimensional Likelihood Test – continued

ZEUS 94-96



2-Dimensional Likelihood Test – continued

Likelihood Distributions



Conclusions

1. We have searched for deviations from Standard Model expectations in $eP \rightarrow eX$ scattering at high Q^2 and high x .
 - The Neutral Current DIS cross section predictions are known to an accuracy at the level of 6%.
 - The events are experimentally very clean. There are no significant backgrounds.
2. In a sample with integrated luminosity 20.1 pb^{-1} , we find:
 - 2 events with $Q^2 > 35000 \text{ GeV}^2$ where only 0.145 ± 0.013 are expected, corresponding to a Poisson probability of 0.96 %.
 - 4 events for ($x > 0.55, y > 0.25$) where only 0.91 ± 0.08 are expected, corresponding to a Poisson probability of 1.4 %.

An analysis using a large ensemble of simulated Standard Model experiments indicates that statistical fluctuations at these levels would occur

 - at *some* Q^2 for ($Q^2 > 5000 \text{ GeV}^2$) in 6 % of all experiments;
 - at *some* x for ($y > 0.25, Q^2 > 5000 \text{ GeV}^2$) in 7.6 % of all experiments.
3. A likelihood analysis sensitive to the event distribution in (x, y) gives probabilities of
 - 0.72 % for the events in the region ($x > 0.55, y > 0.25$),
 - 50.2 % for the events in the region ($x > 0.05, y > 0.05$), excluding the region ($x > 0.55, y > 0.25$), indicating that the data are in good agreement with Standard Model expectations at lower x and Q^2 .
4. The effect is particularly interesting because it occurs in an unexplored kinematic region.